The American Journal of Human Genetics, Volume *106*

Supplemental Data

TTC12 Loss-of-Function Mutations Cause Primary Ciliary Dyskinesia and Unveil Distinct Dynein Assembly Mechanisms in Motile Cilia Versus Flagella

Lucie Thomas, Khaled Bouhouche, Marjorie Whitfield, Guillaume Thouvenin, Andre Coste, Bruno Louis, Claire Szymanski, Emilie Bequignon, Jean-François Papon, Manon Castelli, Michel Lemullois, Xavier Dhalluin, Valérie Drouin-Garraud, Guy Montantin, Sylvie Tissier, Philippe Duquesnoy, Bruno Copin, Florence Dastot, Sandrine Couvet, Anne-Laure Barbotin, Catherine Faucon, Isabelle Honore, Bernard Maitre, Nicole Beydon, Aline Tamalet, Nathalie Rives, France Koll, Estelle Escudier, Anne-Marie Tassin, Aminata Touré, Valérie Mitchell, Serge Amselem, and Marie Legendre

A

```
TTC12a_WT                GAGCACTTTTACGCATAAGAAATGGGAATATTATACAAGTTCAGAAGAAGAAATTGAATC  60
TTC12a_RNAi_resistant    GAGCACGTTTACTCATAAAAAATGGGAATACTATACATCATCAGAAGAGGAAATCGAATC  60
                         ****** ***** ***** ********** ******   ******** ***** *****

TTC12a_WT                TGAGCCAATAGTTCCTAAAGATGACCCAAATTTCAGAGCCTTAGAATTAGATATGGAATA  120
TTC12a_RNAi_resistant    AGAGCCTATTGTTCCAAAAGACGATCCTAACTTTAGAGCTTTGGAATTGGATATGGAGCA  120
                          ***** ** ***** ***** ** ** ** ** ***** ** ***** ********  *

TTC12a_WT                AAGAAAGAAAAAGAAAGAGGAAGACATGAAAAAGGCAGAGGAATTGAAAAACAAAGGCAA  180
TTC12a_RNAi_resistant    AAGAAAAAAGAAAAAGGAAGAGGATATGAAGAAAGCTGAAGAGTTAAAGAATAAGGGCAA  180
                         ****** ** ** ** ** ** ** ***** ** ** ** ** ** ** ** ** *****

TTC12a_WT                TGAGTATTATAGTAAGGGTGATTATGATCATGCGGCTTGGAAATATTCTTAAGCCCTTGA  240
TTC12a_RNAi_resistant    CGAATATTACTCAAAAGGAGATTATGATCACGCTGCGTGGAAGTATTCATAAGCTTTGGA  240
                          ** *****    ** ** ********** ** ** ***** ***** *****  * **

TTC12a_WT                ATTAGTAAAGGATAATAAGACTTTGTGGTTAAATC     275
TTC12a_RNAi_resistant    ATTGGTTAAAGATAACAAGACATTATGGTTGAACC     275
                         *** ** ** ***** ***** ** ***** ** *
```

212/275 (77.09%)

B

```
TTC12a_WT                STFTHKKWEYYTSSEEEIESEPIVPKDDPNFRALELDMEQRKKKKEEDMKKAEELKNKGN  60
TTC12a_RNAi_resistant    STFTHKKWEYYTSSEEEIESEPIVPKDDPNFRALELDMEQRKKKKEEDMKKAEELKNKGN  60
                         ************************************************************

TTC12a_WT                EYYSKGDYDHAAWKYSQALELVKDNKTLWLN  91
TTC12a_RNAi_resistant    EYYSKGDYDHAAWKYSQALELVKDNKTLWLN  91
                         ********************************
```

91/91 (100%)

Figure S1. *P. tetraurelia* nucleic acid and protein sequences of TTC12a versus TTC12a RNAi-resistant

DNA (A) and protein (B) alignments from ClustalOmega of the target of RNAi (275pb) for WT TTC12a and RNAi-resistant TTC12a. Fully conserved residue (*).

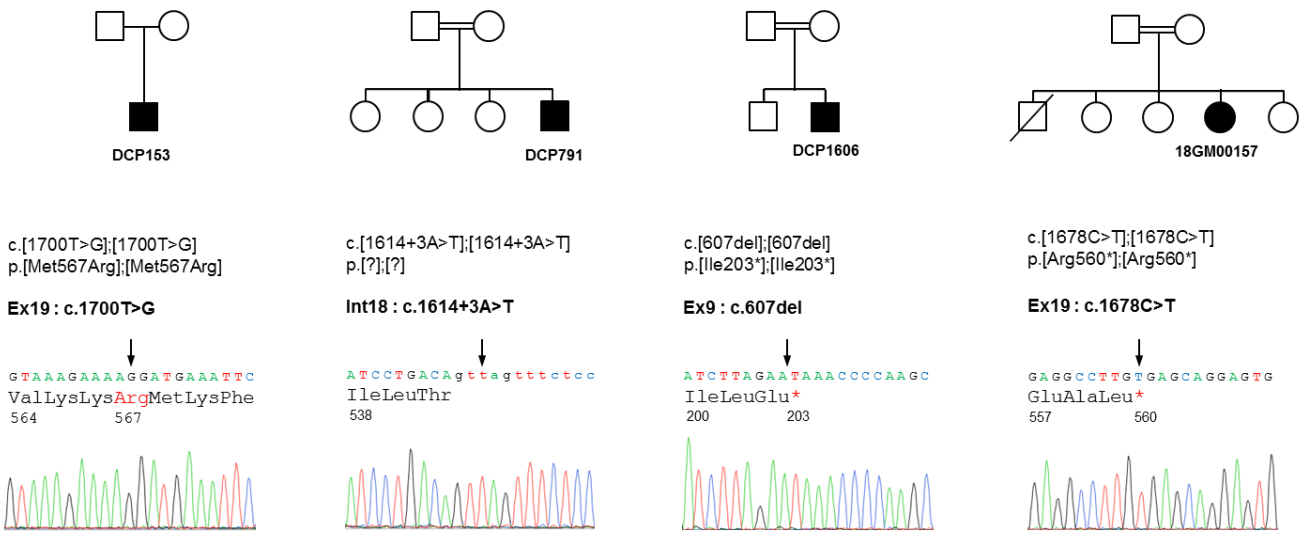

Figure S2. *TTC12* mutations identified in the four independent families

Top: Genealogical trees. Full symbols indicate primary ciliary dyskinesia. All but one individual (DCP153) were born to known consanguineous unions. Bottom: Electrophoregrams showing the *TTC12* mutations identified in the four unrelated PCD probands.

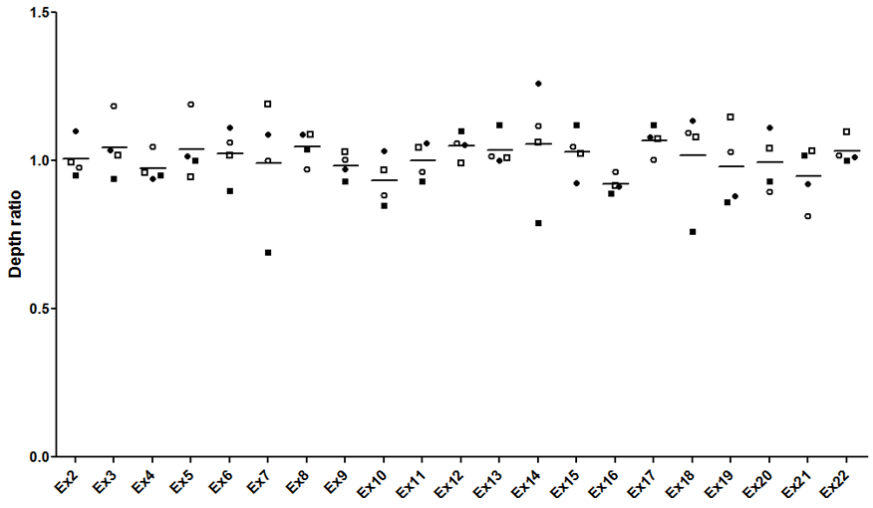

Figure S3. *TTC12* NGS depth ratio analysis

TTC12 copy-number variation analysis in subjects DCP153 (black square), DCP791 (empty square), DCP1606 (black circle), and 18GM00157 (empty circle) by depth ratio analysis of NGS data for each targeted capture probe.

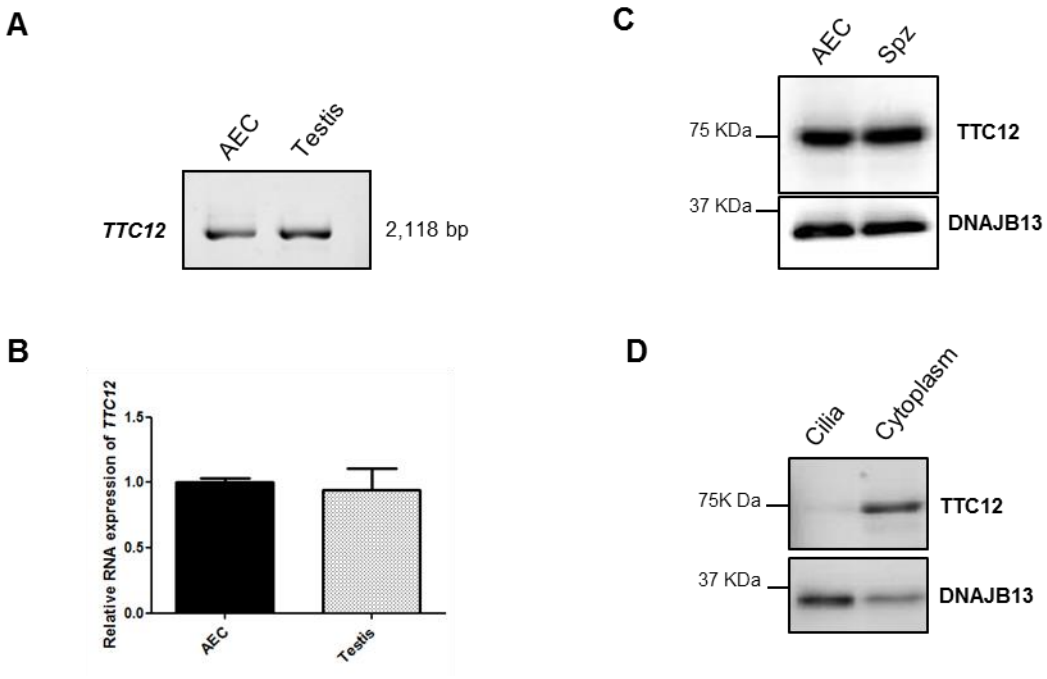

Figure S4. Expression of *TTC12*/TTC12 in human airway epithelial cells (AECs) and testis/spermatozoa in subcellular fractions of AECs

A) Analysis of *TTC12* transcripts in AECs and testis by RT-PCR followed by Sanger sequencing showing a unique isoform present in both cell types corresponding to the 705-residue protein (2,118 bp PCR-product, NM_017868.4).

B) Similar levels of *TTC12* transcripts in AECs and testis tissue, as determined by RT-qPCR with *ERCC3* as endogenous control. Data are represented as the mean ± SEM with no significant differences using *t*-test, p>0.1 (n=8).

C) Detection of the TTC12 protein in AECs and spermatozoa by western blot. DNAJB13, a component of radial spokes, was used as positive control (the expected mass of the TTC12 protein is 78KDa).

D) Cytoplasmic expression of TTC12 in AECs. AECs were fractioned and analyzed by western blot. TTC12 appears to be mainly cytoplasmic, whereas DNAJB13, a component of radial spokes used as control, was found mainly in the cilia fraction.

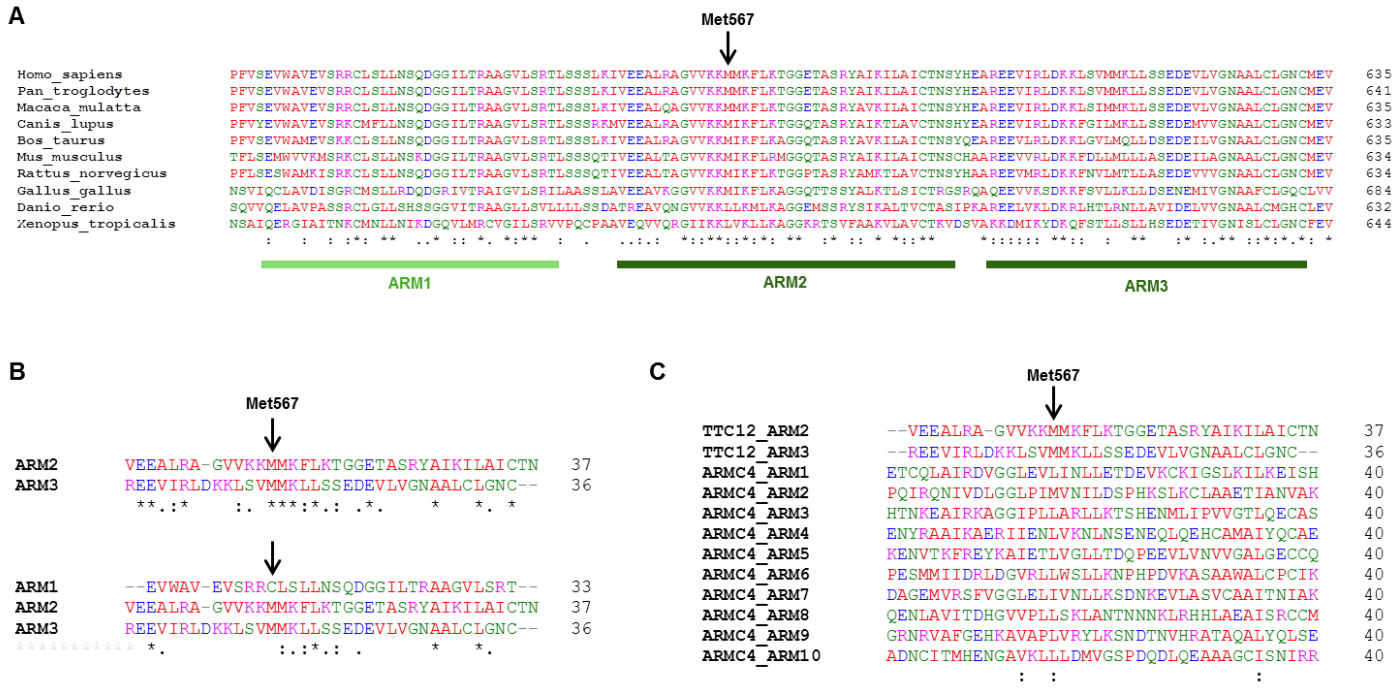

Figure S5. Evolutionary conservation of TTC12 ARM domains and Met567

A) Partial sequence alignment of TTC12 proteins from several species shows the evolutionary conservation of the three ARM domains, including the Met567-flanking region located in ARM2 (residue mutated in individual DCP153). The dark green lines represent conserved domains ARM2 and ARM3; the light green line represents the degenerated ARM1 domain.

B) Sequence alignment of TTC12 ARM2 and ARM3 domains compared to the alignment of ARM1, ARM2 and ARM3 domains confirms the high homology between ARM2 and ARM3 as compared to the degenerated ARM1 domain that has lost 7 of the 11 fully conserved residues found in ARM2 and ARM3. The Met567 residue in the ARM2 domain is conserved in the ARM3 domain.

C) Sequence alignment of TTC12 ARM2 and ARM3 domains with the 10 ARM domains found in ARMC4 (PCD gene) shows the conservation of a hydrophobic residue at position corresponding to Met567 in TTC12.

Fully conserved residue (*); residues with strongly similar properties (:); residues with similar properties (.)

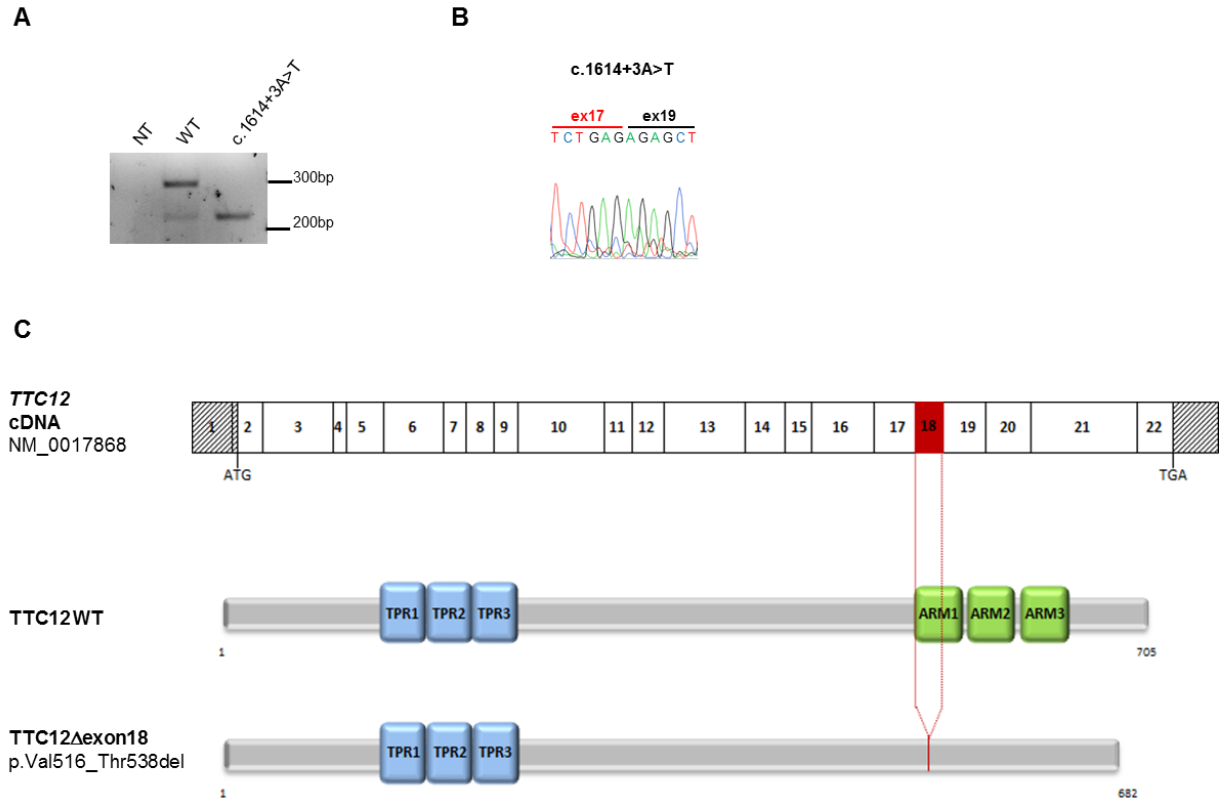

Figure S6. The *TTC12* c.1614+3A>T mutation identified in individual DCP791: Functional consequences on *TTC12* RNA splicing and predicted impact at the protein level

A) RT-PCR amplification of *TTC12* transcripts obtained from HEK293 cells transfected with a minigene containing a genomic DNA region spanning exons 17 to 19 of *TTC12*, with or without the c.1614+3A>T mutation. A representative gel picture shows bands corresponding to fully spliced *TTC12* transcripts (296 bp) and a smaller molecular species (227 bp) corresponding to *TTC12* transcripts lacking exon 18 (*TTC12*-Δexon18). The low amounts of *TTC12*-Δexon18 transcripts also detected with the WT construct may result from the strong overexpression of the minigene in this transient expression study. NT: non-transfected cells

B) Sanger sequencing of RT-PCR products generated from HEK293 cells transfected with the mutated *TTC12* minigene confirming the complete skipping of exon 18 in *TTC12* transcripts.

C) Schematic representation of the predicted impact of exon 18 skipping at the protein level. Exonic organization of the human *TTC12* cDNA (top) and domain-organization model of wild-type TTC12 and

TTC12 deleted from the domain encoded by exon 18 (bottom) according to CDD NCBI database. No ARM domain is predicted in the TTC12 protein lacking amino acids encoded by exon18. TPR: tetratricopeptide repeat; ARM: armadillo repeat.

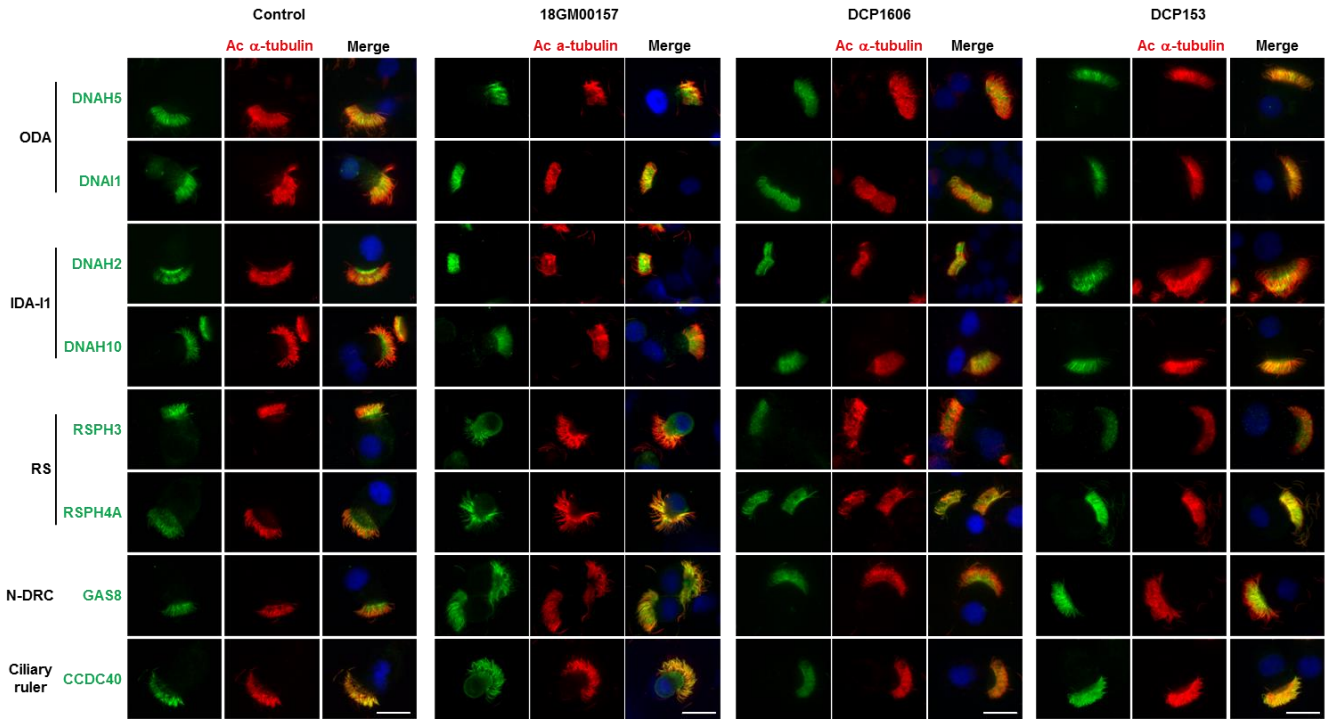

Figure S7. Expression of ODA, IDA, RS, N-DRC and ciliary ruler markers in AECs from individuals with *TTC12* mutations

Immunofluorescence microscopy analyses of airway epithelial cells from PCD individuals 18GM00157, DCP1606 and DCP153 are shown. Immunostaining of the main axonemal component markers (all in green) and of acetylated α-tubulin (in red) shows a normal expression and localization of all the components tested. Nuclear staining was performed with DAPI (blue). Scale bars, 25 µm. ODA: outer dynein arms; IDA: inner dynein arms; RS: radial spokes; N-DRC: nexin-dynein regulatory complex.

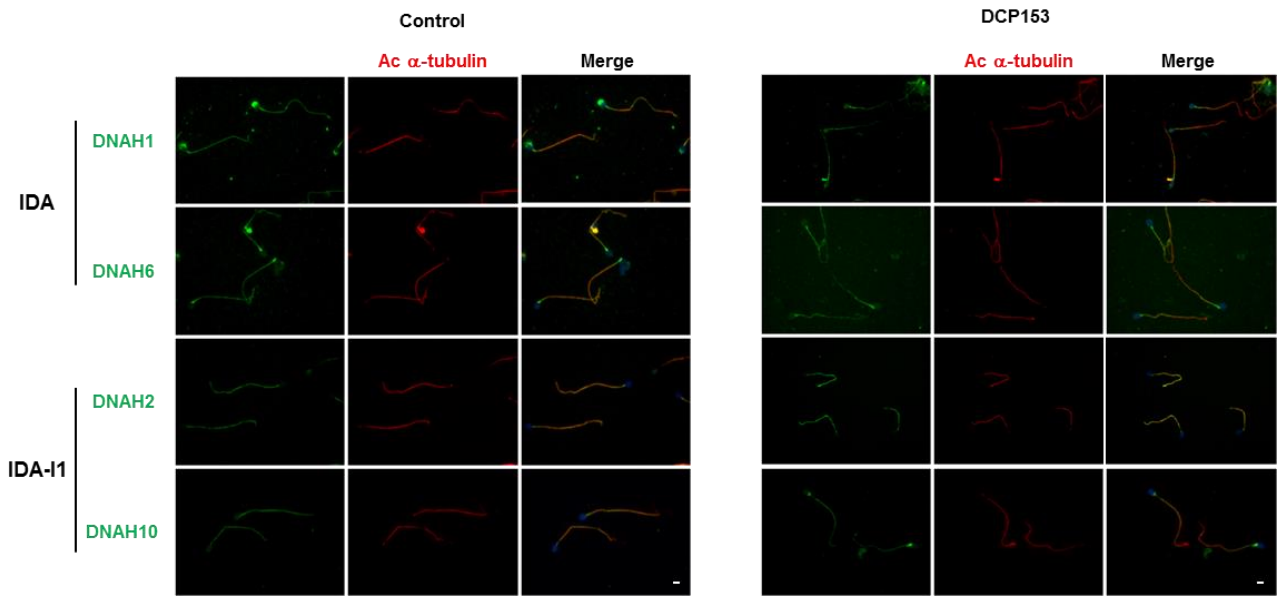

Figure S8. Expression of IDA and IDA-I1 markers in spermatozoa from individual DCP153

Immunofluorescence microscopy analyses in spermatozoa from the infertile PCD individual DCP153. Immunostaining with anti-DNAH1 and anti-DNAH6 antibodies (markers of IDA subspecies d and g, respectively) and anti-DNAH2 and anti-DNAH10 antibodies (markers of IDA-I1), all in green, together with α–tubulin (in red) shows a normal expression and localization of all the components tested. Nuclear staining was performed with DAPI (blue). Scale bars, 5 µm. IDAs: inner dynein arms.

Figure S9. **Orthologs of human TTC12 in *Paramecium tetraurelia***

A) Domain organization model of human TTC12 protein compared to TTC12a and TTC12b from *P. tetraurelia,* according to SMART webtool, CDD NCBI database and Interpro software. TTC12a and TTC12b are two closely related paralogs resulting from the last two whole-genome duplications.

B) TTC12 protein interspecies alignments from ClustalOmega. Fully conserved residue (*); residues with strongly similar properties (:); residues with similar properties (.)

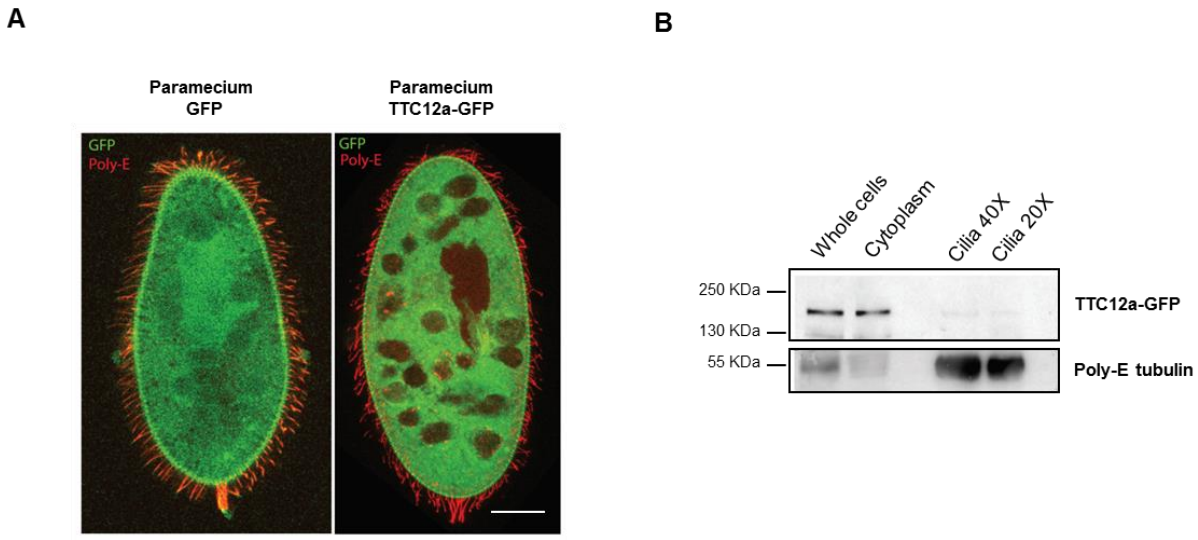

Figure S10. Localization of TTC12a in *Paramecium tetraurelia*

A) Paramecia expressing either GFP (left panel) or TTC12a-GFP (right panel) show a very high level of cytoplasmic GFP staining. Scale bar, 20 μm.

B) Cytoplasmic expression of TTC12a in paramecia. Protein extracts from whole cells, cytoplasm (cell body of deciliated cells) or cilia fraction of the same cells loaded with a 40- or 20-fold excess of cilia (40X, 20X), were probed with anti-GFP and anti-Poly-E tubulin antibodies. TTC12a is present in the cytoplasm, whereas the protein is almost not detected in the cilia fraction.

A

	Position	Sequence	Efficiency
gRNA 1	Exon 3	AAAGAGACTACTGCTTATGG	82%
gRNA 2	Exon 3	ACTGCTTATGGAGGAAGACC	60%

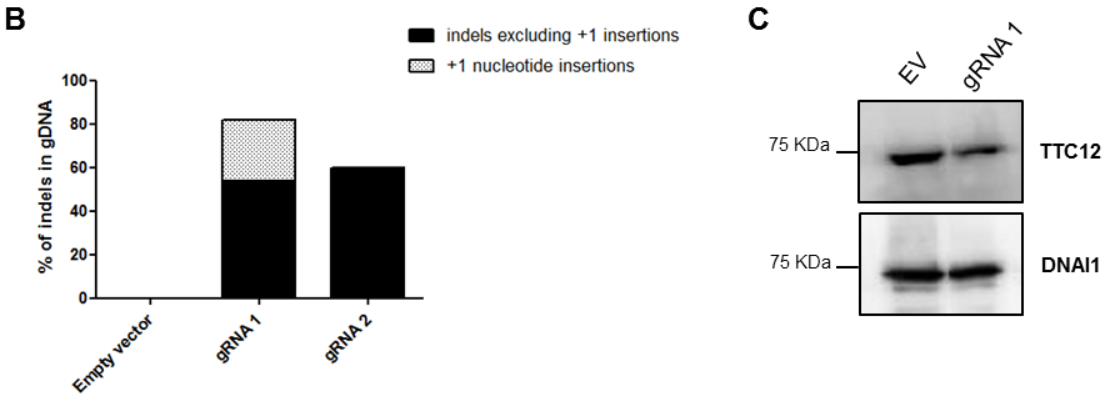

Figure S11. Insertions and deletions (indels) in *TTC12*-CRISPR transduced AECs

A) Sequence, position and efficiency of two CRISPR guides targeting *TTC12*.

B) Percentage of insertions and deletions (indels) in the genomic DNA of *TTC12*-CRISPR AECs compared to control AECs (transduced with an empty vector). Sanger sequencing was performed and analyzed with the TIDE webtool. Guide 1 has a better efficiency (82% of indels) than guide 2 (60% of INDELS). Grey = proportion of +1 single nucleotide insertions (28% with guide 1, and 1% with guide 2).

C) Western blot of cells lysates from AECs in which *TTC12* has or not been invalidated by a CRISPR-Cas9 approach, showing a decreased expression of TTC12 in the invalidated culture.

gDNA: genomic DNA; AECs: airway epithelial cells; EV: empty vector.

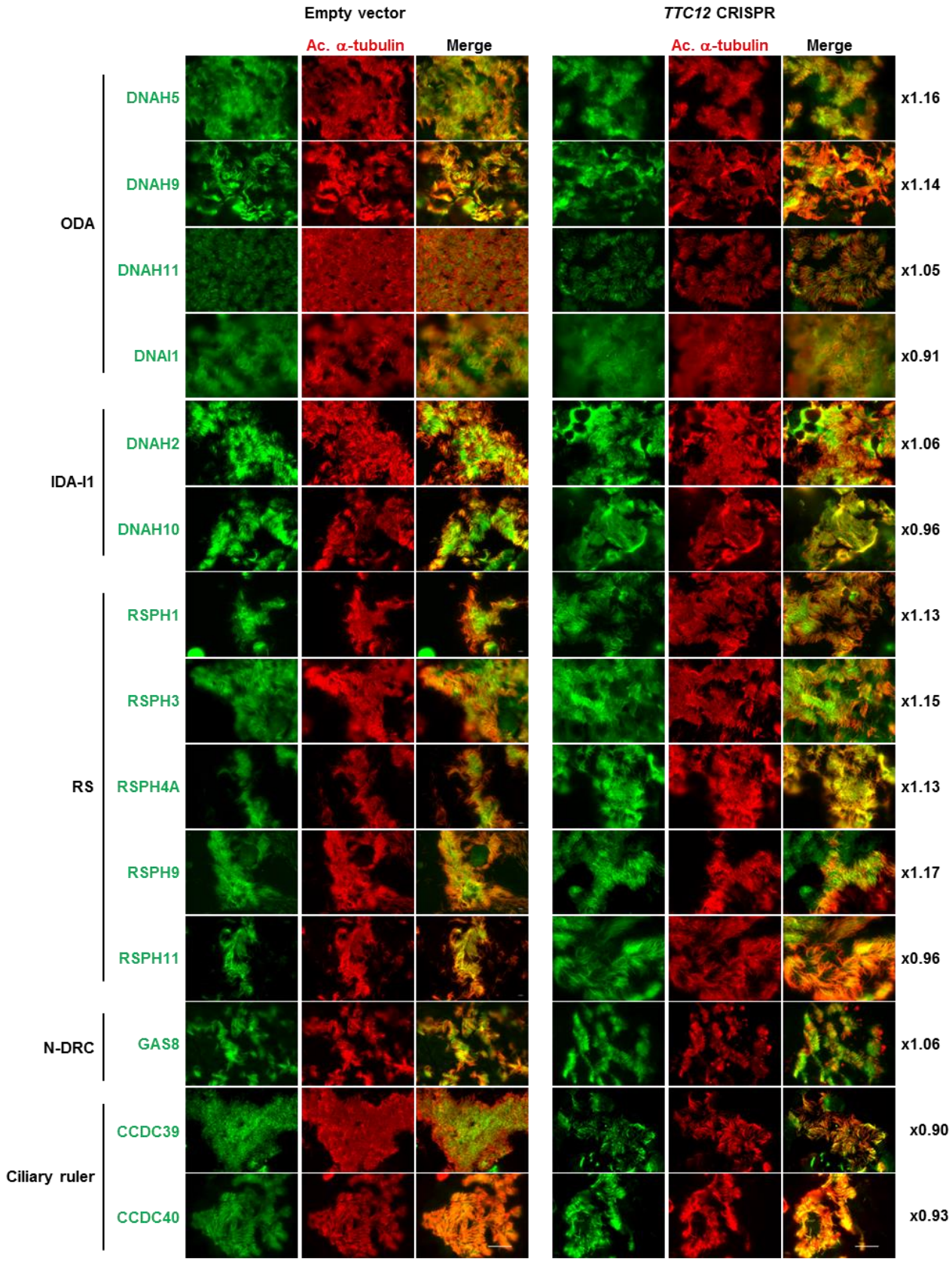

Figure S12. Expression of ODA, IDA, RS, N-DRC and ciliary ruler markers in AEC cultures in which *TTC12* has or not been invalidated by a CRISPR-Cas9 approach

Immunostaining of the main axonemal component markers (all in green) and of the acetylated α-tubulin (in red) in AECs invalidated for *TTC12* shows an expression similar to that found in native AECs. Scale bars, 25 µm. Green labeled areas were measured with ImageJ software and normalized against the tubulin labeled area (red). The dynein/tubulin ratios obtained in *TTC12*-CRISPR transduced cells were then normalized to ratios obtained in EV-transduced cells before. Values of those final ratios are indicated on the right side of the figure and showed no differences between green and red labels.

ODA: outer dynein arm; IDA: inner dynein arm; RS: radial spoke; N-DRC: nexin-dynein regulatory complex; EV: empty vector.

Table S1: Primers sequences

PCR and Sanger sequencing		
Name	**Sequence**	**PCR product size (bp)**
TTC12_ex9F	ACTGGGAGCAGGAGGAGG	315
TTC12_ex9R	GACCCAACTGTGCAGGAAAG	
TTC12_ex18F	TTAGGGGAGACAGACATGGG	465
TTC12_ex18R	GGACACAGCAAGGAGGTCAC	
TTC12_ex19F	TGGCAAGGGGCTATGATTAC	448
TTC12_ex19R	AAGCAAATCCCTATCCAAGAAG	
Reverse-Transcription PCR and Real Time PCR		
Name	**Sequence**	**PCR product size (bp)**
TTC12exon2_ATG	GATTCCGGTTCACAATGGATGC	2118 (NM_017868.4)
TTC12exon22_STOP	TTAGCATAGGAACAACACACGGT	
QPCR_TTC12-Ex11F	TGACAACGAGGTCATAAGAAGG	68
QPCR_TTC12-Ex12R	CAGACCATTTCTTCAACTGCAT	
QPCR_ERCC3-Ex9F	ACTGGATGGAGCTGCAGAAT	70
QPCR_ERCC3-Ex10R	GACATAGGGCACCAGACCTC	
Minigene construct		
Name	**Sequence**	**PCR product size (bp)**
MinigeneTTC12_17F	ATGTGTCTTCAGGCTCCCTTTGT	3035
MinigeneTTC12_19R	TCACAAGGCCTCCTCAACAATTT	
pCDNA3topo_3'UTR_F	GAGCTCGGATCCACTAGTCC	296
pCDNA3topo_5'UTR_R	GGAGAGGGTTAGGGATAGGC	
Guides RNA and on-target PCR		
Name	**Sequence**	**PCR product size (bp)**
TTC12gRNA1_lentiCRISPRv2F	CACCGAAAGAGACTACTGCTTATGG	/
TTC12gRNA1_lentiCRISPRv2R	AAACCCATAAGCAGTAGTCTCTTTC	
TTC12gRNA2_lentiCRISPRv2F	CACCGACTGCTTATGGAGGAAGACC	/
TTC12gRNA2_lentiCRISPRv2R	AAACGGTCTTCCTCCATAAGCAGTC	
PCR_Ontarget_F	TGACCCAGTTGTGCAACAGA	364

Table S2: Antibodies used for immunofluorescence microscopy studies

Antibody	Localization	Host	Clonality	Company	Reference	Dilution	
						Cilia	Flagella
α acetylated tubulin	Microtubulin doublets	mouse	monoclonal	Sigma	(6-11-B1) T6793	1/600	/
α tubulin	Microtubulin doublets	mouse	monoclonal	Sigma	T9026	/	1/500
CCDC39	Ciliary ruler (IDA-RS-NDRC linker)	rabbit	polyclonal	Sigma	HPA035364	1/400	/
CCDC40	Ciliary ruler (IDA-RS-NDRC linker)	rabbit	polyclonal	Sigma	HPA022974	1/500	/
DNAH1	IDA heavy chain, subspecies d	rabbit	polyclonal	Sigma	HPA036805	1/50	1/25
DNAH2	IDA-I1 heavy chain	rabbit	polyclonal	Sigma	HPA067103	1/100	1/50
DNAH3	IDA heavy chain, subspecies a? b? c? e?	rabbit	monoclonal	Abcam	ab172632	1/50	1/50
DNAH5	ODA g heavy chain	rabbit	polyclonal	Sigma	HPA037470	1/200	NR
DNAH6	IDA heavy chain, subspecies g	rabbit	polyclonal	Sigma	HPA036391	1/50	1/50
DNAH8	ODA g heavy chain	rabbit	polyclonal	Sigma	HPA028447	NR	1/2000
DNAH9	ODA b heavy chain, distal	rabbit	polyclonal	Sigma	HPA052641	1/150	NR
DNAH10	IDA-I1 heavy chain	rabbit	polyclonal	Sigma	HPA039066	1/150	1/50
DNAH11	ODA b heavy chain, proximal	rabbit	polyclonal	Sigma	HPA045880	1/75	NR
DNAH12	IDA heavy chain, subspecies a? b? c? e?	rabbit	polyclonal	Sigma	HPA058203	1/50	1/50
DNAH17	ODA b heavy chain, distal	rabbit	polyclonal	Sigma	HPA024354	NR	1/200
DNAI1	ODA intermediate chain	rabbit	polyclonal	Sigma	HPA021649	1/300	1/200
DNALI1	IDA associated protein, subspecies a/c/d	rabbit	polyclonal	Sigma	HPA028305	1/150	1/100
GAS8	DRC4	rabbit	polyclonal	Sigma	HPA041311	1/300	/
RSPH1	Radial Spoke Head	rabbit	polyclonal	Sigma	HPA017382	1/100	/
RSPH11	Radial Spoke Stalk	rabbit	polyclonal	Sigma	HPA039193	1/200	/
RSPH3	Radial Spoke Stalk	rabbit	polyclonal	Novus	NBP1-84244	1/100	/
RSPH4A	Radial Spoke Head	rabbit	polyclonal	Sigma	HPA031196	1/200	/
RSPH9	Radial Spoke Head	rabbit	polyclonal	Sigma	HPA031703	1/200	/

NR: Not Relevant

Table S3: Position and length of DNA segments used in paramecia feeding experiments

Gene	Position	Length (bp)
TTC12a	[471-745]	275
TTC12b	[471-588]-[613-745]	251

Table S4: High-speed videomicroscopy parameters

Individuals	**Beating cilia (%)**	**CBF (Hz)**	**Angle (°)**	**Distance travelled by the cilum tip (µm/sec)**
18GM00157	30	10 ± 3.3	50 ± 24	57.3 ± 42.4
DCP1606	50	11.4 ± 5.4	31 ± 21	36.9 ± 26.2
DCP153	90	6.3 ± 2.0	50 ± 22	39.1 ± 43.2
Controls (mean ± SD)[a]	91 ± 13	8.9 ± 2.0	71.6 ± 6.6	66.7 ± 14.2
P[b], n=15	0.027	ns	0.002	0.04

CBF: ciliary beat frequency, SD: standard deviation, ns: not significant. Angle and distance travelled were evaluated on beating cilia.

[a] *According to the normal values published in reference*[1]

[b] *using the Mann-Whitney U test, with 15 individuals with non PCD bronchiectasis; p<0.05 was considered as significant.*

Table S5: Allele frequency of *TTC12* mutations identified in individuals

Individuals	**Genomic position (Grch37)**	**Mutation**	**Exon**	**Mutation type**	**GnomAD allele frequency (mutated/total allele number)**	**Number of homozygotes**
DCP1606	chr11:113209524	c.607del p.Ile203*	9	Nonsense	0	0
DCP791	chr11:113230733	c.1614+3A>T p.?	Intron 18	Splice (exon 18 skipping)	0	0
18GM00157	chr11:113233186	c.1678C>T p.Arg560*	19	Nonsense	$4x10^{-5}$ (14/282804)	0
DCP153	chr11:113233208	c.1700T>G p.Met567Arg	19	Missense	$6x10^{-5}$ (17/282758)	0

Table S6: Expression pattern of *Paramecium tetraurelia TTC12* genes

Gene	Accession number	Expression pattern[a]		Protein length	Identity (%)
		Life cycle	Deciliation/Reciliation		
TTC12a	PTET.51.1.G1640129	High	Overexpressed	846 residues	83.45
TTC12b	PTET.51.1.G1420106	Basal	Not modified	850 residues	

[a] *according to ParameciumDB*

SUPPLEMENTAL MATERIAL AND METHODS

High-speed videomicroscopy

Ciliated samples were obtained by nasal brushing with a 2 mm cytology brush (Laboratoires Gyneas). Cells were suspended in B1 BSA medium (CCD Lab) and examined within three hours after sampling. All observations were performed at room temperature with an inverted microscope (Axiovert 200, Carl Zeiss S.A.S.) with an oil immersion x100 objective, and within 20 min. Beating ciliated edges were recorded with a digital camera (PixeLINK A741) at a rate of 355 frames per second. Each movie was composed of 1,800 frames with a definition of 256 × 192 pixels. Pixel size was (0.13 × 0.13) μm^2. Twenty distinct areas containing intact undisrupted ciliated epithelial edges devoid of mucus and beating in the plane of the camera were recorded. Qualitative and quantitative evaluations of ciliary beat patterns were performed as previously described[1]. Briefly, 10 beating cilia individualized were followed during a complete beating cycle (one cilium selected per video/edges) in order to measure the following parameters: ciliary beat frequency (CBF), beating angle and distance travelled by the cilium tip per second. These results were compared to a disease control group previously published (i.e., 15 individuals with non-PCD bronchiectasis[1]) using the Mann-Whitney U test; $p<0.05$ was considered as significant.

Quantitative RT-PCR

One microgram of total RNA from airway cells at cultured at air-liquid interface or testis tissue (Takara Bio Europe/Clontech) was extracted using the RNeasy Mini Kit (Qiagen) and then subjected to reverse transcription with the Reverse Transcriptor kit (Roche) following the manufacturer's instructions. The real-time PCR assays were performed in the Light Cycler LC480 (Roche) with the mesablue qPCR mastermix Plus for Sybr Assay (Eurogentec). *ERCC3*, an ubiquitously expressed gene, was used as an endogenous control to normalize the data and determine the relative expression between AECs and testis by calculating the primer efficiency$^{-\Delta\Delta Ct}$. The primers used are listed in **Table S1**.

Cilia isolation from ALI cultures

After more than 21 days of culture of AECs in ALI conditions (as indicated above), cilia isolation was performed as described[2]. Briefly, the apical surface of AEC cultures was washed two times with PBS before being gently swirled with a deciliation buffer (10mM Tris-HCL pH7.5, 50mM NaCl, 10mM CaCl2, 1mM EDTA, 0.1% Triton X100, 7mM Bmercaptoethanol, 1% Protease inhibitor). The cilia fraction was collected and first centrifugated 1 min at 1000 g at 4°C, then 5 min at 12000g at 4°C to gather all cilia that were then resuspended in resuspension buffer (30mM HEPES pH7.3, 25mM NaCl, 5mM MgSO4, 1mM EGTA, 0.1mM EDTA, 1mM DTT, 1% protease inhibitor). The fraction remaining on the insert was considered as the cytoplasmic part. Both fractions were suspended in ice-cold lysis buffer to perform immunoblotting as described in the Material and Methods section of the main text.

Minigene constructs and *in vitro* expression

Genomic DNA was extracted from blood obtained from a healthy control and from DCP791 individual carrying the c.1614+3A>T splice site mutation. A region spanning exons 17 to 19 containing or not the c.1614+3A>T transversion was amplified by PCR from those genomic DNAs and cloned into pcDNA3.1/V5-His-TOPO using the TOPO TA cloning kit (Thermofischer Sc.) according to the manufacturer's recommendations.

Constructs were checked by Sanger sequencing before being transfected in HEK293 cells with FuGENE® HD Transfection Reagent (Promega). Total RNA was extracted with RNeasy Mini Kit (Qiagen) before being treated with Dpn1 to eliminate the bacterial plasmid. Reverse transcription was then performed with the Reverse Transcriptor kit (Roche) following the manufacturer's instructions. To avoid the amplification of HEK293 endogenous *TTC12* transcripts, PCR was performed with primers located in the plasmidic 5' and 3' untranslated regions flanking the *TTC12* gene fragment. All primers used are listed in **Table S1**.

CRISPR-cas9 guides design and lentiviral vector construct

Oligonucleotides coding for guide RNAs that target the third exon of *TTC12* were designed with the crispor.tefor.net webtool. We selected two guides, consisting of 20-bp sequences followed by NGG PAM of the CRISPR/SpCas9, that combined the higher specificity score associated with the lower out-of-frame score. We previously checked the absence of off-targets in introns or exons of genes known to be implicated in PCD, and that all off-targets contained more than three single-nucleotide mismatches. Guides were cloned into plentiCRISPRv2, a gift from Feng Zhang[3] (Addgene plasmid # 52961; http://n2t.net/addgene:52961; RRID:Addgene_52961) according to the original online protocol of the Zhang lab (https://www.addgene.org/static/data/plasmids/52/52961/52961-attachment_B3xTwla0bkYD.pdf). The production of lentiviruses was performed by AniRA Vectorologie (SFR Biosciences Gerland – Lyon Sud). Guides and primers used are listed in **Table S1**.

1. Papon, J.-F., Bassinet, L., Cariou-Patron, G., Zerah-Lancner, F., Vojtek, A.-M., Blanchon, S., Crestani, B., Amselem, S., Coste, A., Housset, B., et al. (2012). Quantitative analysis of ciliary beating in primary ciliary dyskinesia: a pilot study. Orphanet J Rare Dis *7*, 78.

2. Ostrowski, L.E. (2006). Chapter 14 - Preparation of Cilia from Human Airway Epithelial Cells. In Cell Biology (Third Edition), J.E. Celis, ed. (Burlington: Academic Press), pp. 99–102.

3. Sanjana, N.E., Shalem, O., and Zhang, F. (2014). Improved vectors and genome-wide libraries for CRISPR screening. Nat Methods *11*, 783–784.